

Tm³⁺-doped CW fiber laser based on a highly GeO₂-doped dispersion-shifted fiber

V. V. Dvoyrin,^{1,2} I. T. Sorokina,² V. M. Mashinsky,¹ L. D. Ischakova,¹ E. M. Dianov,¹
V. L. Kalashnikov,^{3,*} M. V. Yashkov,⁴ V. F. Khopin,⁴ A. N. Guryanov⁴

¹Fiber Optics Research Center, Russian Academy of Sciences, 38 Vavilov Street, 119333 Moscow, Russia

²Department of Physics, Norwegian University of Science and Technology, N-7491 Trondheim, Norway

³Institut für Photonik, TU Wien, Gusshausstrasse 27/387, A-1040 Vienna, Austria

⁴Institute of Chemistry of High-Purity Substances, Russian Academy of Sciences, 49 Tropinin Street, 603600 Nizhny Novgorod, Russia

*kalashnikov@tuwien.ac.at

Abstract: A novel all-fiber laser based on a highly GeO₂-doped dispersion-shifted Tm-codoped fiber, pumped at 1.56 μm wavelength and lasing at 1.862 μm wavelength with a slope efficiency up to 37% was demonstrated. The single-mode Tm-doped fiber with the 55GeO₂-45SiO₂ core was fabricated for the first time by MCVD technique. The laser produces spectral side bands, resulting from the four-wave mixing owing to the shift of the zero-dispersion-wavelength of the fiber to the laser wavelength, thus, making it potentially particularly attractive for dispersion management and ultrashort pulse generation.

©2011 Optical Society of America

OCIS codes: (060.2290) Fiber materials; (060.2320) Fiber optics amplifiers and oscillators.

References and links

1. "Rare-Earth-Doped Fiber Lasers and Amplifiers," M. J. E. Dignonet, ed. Marcel Dekker, Inc., New York-Basel, 2001.
2. S. D. Jackson, and T. A. King, "High-power diode-cladding-pumped Tm-doped silica fiber laser," *Opt. Lett.* **23**(18), 1462–1464 (1998).
3. S. D. Jackson, "Midinfrared holmium fiber lasers," *IEEE J. Quantum Electronics* **42**(2), 187–191 (2006).
4. A. S. Kurkov, V. V. Dvoyrin, and A. V. Marakulin, "All-fiber 10 W holmium lasers pumped at λ=1.15 microm," *Opt. Lett.* **35**(4), 490–492 (2010).
5. H. Osanai, T. Shioda, T. Moriyama, S. Araki, M. Horiguchi, T. Izawa, and H. Takata, "Effect of Dopants on Transmission Loss of Low-OH-Content Optical Fibers," *Electron. Lett.* **12**(21), 549–550 (1976).
6. S. H. Wemple, "Material dispersion in optical fibers," *Appl. Opt.* **18**(1), 31–35 (1979).
7. T. Sun, G. Kai, Zh. Wang, Sh. Yuan, and X. Dong, "Enhanced nonlinearity in photonic crystal fiber by germanium doping in the core region," *Chin. Opt. Lett.* **6**(2), 93–95 (2008).
8. J. Wang, J. R. Lincoln, W. S. Brocklesby, R. S. Deol, C. J. Mackechnie, A. Pearson, A. C. Tropper, D. C. Hanna, and D. N. Payne, "Fabrication and optical properties of lead-germanate glasses and a new class of optical fibres doped with Tm³⁺," *J. Appl. Phys.* **73**(12), 8066–8075 (1993).
9. J. Wu, Z. Yao, J. Zong, and S. Jiang, "Highly efficient high-power thulium-doped germanate glass fiber laser," *Opt. Lett.* **32**(6), 638–640 (2007).
10. V. M. Mashinsky, V. B. Neustruev, V. V. Dvoyrin, S. A. Vasiliev, O. I. Medvedkov, I. A. Bufetov, A. V. Shubin, E. M. Dianov, A. N. Guryanov, V. F. Khopin, and M. Yu. Salgansky, "Germania-glass-core silica-glass-cladding modified chemical-vapor deposition optical fibers: optical losses, photorefractivity, and Raman amplification," *Opt. Lett.* **29**(22), 2596–2598 (2004).
11. V. L. Kalashnikov, "Effective refractive indexes and dispersion characteristics of the tapered fibers," <http://info.tuwien.ac.at/kalashnikov/TFmodes.html>.
12. G. Sansone, G. Steinmeyer, C. Vozzi, S. Stagira, S. De Silvestri, K. Starke, D. Ristau, B. Schenkel, J. Biegert, A. Gosteva, U. Keller, and M. Nisoli, "Mirror dispersion control of a hollow fiber supercontinuum," *Appl. Phys. B* **78**(5), 551–555 (2004).
13. E. Sorokin, V. L. Kalashnikov, J. Mandon, G. Guelachvili, N. Picqué, and I. T. Sorokina, "Cr⁴⁺: YAG chirped-pulse oscillator," *N. J. Phys.* **10**(8), 083022 (2008).
14. V. L. Kalashnikov, E. Podivilov, A. Chernykh, S. Naumov, A. Fernandez, R. Graf, and A. Apolonski, "Approaching the microjoule frontier with femtosecond laser oscillators: theory and comparison with experiment," *N. J. Phys.* **7**, 217 (2005).
15. A. Chong, J. Buckley, W. Renninger, and F. Wise, "All-normal-dispersion femtosecond fiber laser," *Opt. Express* **14**(21), 10095–10100 (2006).

16. S. Lefrançois, K. Kieu, Y. Deng, J. D. Kafka, and F. W. Wise, "Scaling of dissipative soliton fiber lasers to megawatt peak powers by use of large-area photonic crystal fiber," *Opt. Lett.* **35**(10), 1569–1571 (2010).
 17. V. L. Kalashnikov, Energy scalability of mode-locked oscillators: completely analytical approach to an analysis, *Europhysics Conference Abstracts Volume 34C* (4th EPS-QEOD EUROPHOTON Conference on Solid-State, Fibre, and Waveguide Coherent Light Sources held in Hamburg, Germany, 29 August - 3 September 2010), p. TuP4.
-

1. Introduction

The long-wavelength spectral edge of the operational wavelength range of conventional rare-earth-doped silica fiber lasers is known to be around 1.9 μm [1]. Even longer-wavelength range up to 2.15 μm is covered now by Ho-doped fiber lasers [2–4]. Further spectral expansion is expected through the involvement of nonlinear effects, like e.g. Raman scattering. GeO_2 - SiO_2 glass fibers are particularly interesting for infrared laser applications for several reasons. First, as a result of reduced Rayleigh scattering, they exhibit lower optical losses than conventional silica-glass fibers with high SiO_2 content at longer wavelengths [5,6]. Second, they allow an easy variation of dispersion of the fiber by varying the GeO_2 concentration and profile in the core as well as enhancement of the fiber nonlinearity [7]. This opens up opportunities for development in the future of the high energy ultrashort pulsed Tm-laser sources as well as super-continuum sources in the long-wavelength spectral range above 2 microns – which is currently a very attractive, albeit challenging topic.

Silica-free germanate Tm-doped fibers fabricated by other techniques than vapor deposition methods are known [8,9]. The continuous-wave (CW) lasing efficiency of corresponding fiber lasers with bulk mirrors can be high enough, up to ~70%, with output power at 100 W level [9]. At the same time, the group velocity dispersion (GVD) properties of the fiber, important for applications of these fibers in ultrafast optics, have not been addressed in the literature so far.

In this work we introduce an MCVD-fabricated silica-clad Tm-doped fiber with a high concentration of GeO_2 in its core, to provide a zero-dispersion wavelength shifted to the typical spectral region of Tm-doped germanate glasses emission. Besides its good optomechanical properties, expected for silica-rich composition, including a possibility of electrical-fusion splicing, this fiber has such advantages as a high nonlinearity and a zero-dispersion shifted to 1.9 μm area, as well as potentially flattened second order dispersion. Moreover, our theoretical study shows a great flexibility of GVD management in ~2- μm zero-dispersion region in simple step-index germanate-core fibers in contrast to step-index silica fibers, thus, opening way to ultra-short pulse generation and pulse energy scaling.

We also paper report an all-fiber single-mode CW laser based on the Tm-doped fiber with 55 GeO_2 -45 SiO_2 core – a way to compact and practical 2- μm fiber laser sources.

2. Fiber fabrication and experimental

Fiber preform was fabricated by Modified Chemical Vapor Deposition (MCVD) method [10]. Thulium was incorporated to the preform core from the vapor phase. At first stage, a buffer layer of SiO_2 - P_2O_5 -F composition was deposited on the inner surface of the substrate silica tube. Its refractive index matched that one of the silica glass. After, several germanosilicate layers were deposited with a gradual increase of the germanium dioxide concentration up to ~15 mol.%. At this stage a thulium doping from the vapor phase was performed with a raw reagent being metal-organic complex $\text{Tm}(\text{tmhd})_3$. As the last step, the germanate glass forming the core was deposited.

Then, a multi-mode fiber with a core-diameter of approximately 8 μm was drawn from the preform. The concentration of GeO_2 in the fiber core detected by X-ray microanalysis was 55 mol.% (Fig. 1). Tm concentration was close to the detection limit and amounted to 0.2 wt.%. After the fabrication of the multi-mode fiber, a single-mode fiber with a cut-off of 1.43 μm was drawn.

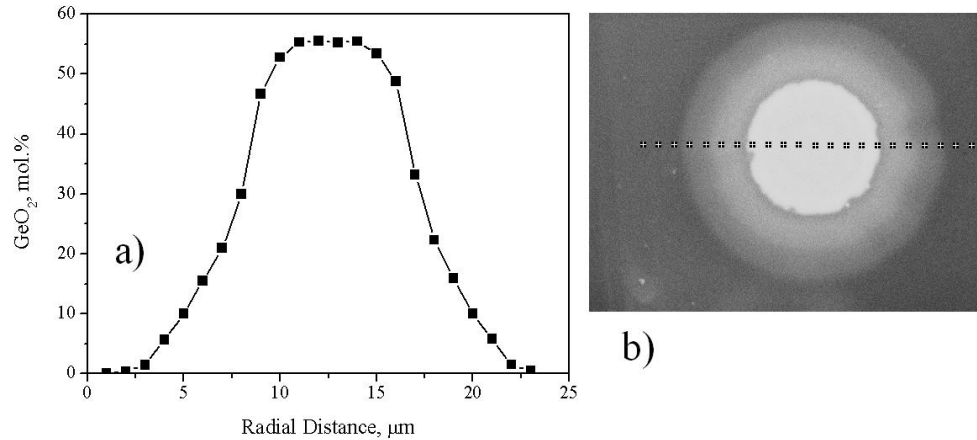


Fig. 1. a) Distribution of GeO₂ in the multi-mode fiber core, b) X-ray photo of the MM fiber core. The points shown on the photo correspond to the points shown in the graphic. The distance between points is 1 μm.

Optical loss spectra were measured by the cut-back technique using a tungsten lamp as the light source. Single-mode CW Er-doped fiber laser ($\lambda = 1.56 \mu\text{m}$) was used to study the fluorescence of the Tm-doped fiber. The amplified spontaneous emission (ASE) of the core-excited Tm-doped was measured from the output end of the fiber.

The laser oscillation was obtained in a linear cavity formed with fiber Bragg gratings (FBG). The FBGs were spliced to the active fiber from both its ends with an electrical fusion splicer. The average splice loss of the active fiber to the fiber Bragg grating was about 0.2 dB, so the fiber is compatible with silica-based fibers. The FBGs were UV-written in a germanosilicate fiber with 20 mol.% concentration of GeO₂ in its core and a cut-off at 1.2 μm wavelength. One FBG was highly reflective (HR) at the 1.862 μm wavelength and the other one (output coupler) has a reflection of 20%. Two Tm-doped fiber pieces of 2.5 and 4.5 m lengths were studied. The fibers were pumped through the HR FBG by the mentioned above Er-doped fiber laser with a pump power up to 210 mW.

The optical spectra were recorded with a double-stage monochromator and a Pb-S photodetector.

3. Results

In what follows we discuss the results of the investigation of the single-mode fiber being interesting for laser applications. Optical loss spectrum of the fiber is presented in Fig. 2. This one has a typical shape of Tm-doped silica glass absorption. A broad absorption band at 1.58 μm suitable for optical pumping is originated from $^3\text{H}_6 \rightarrow ^3\text{F}_4$ transition of Tm³⁺ ion. The small-signal pump absorption at 1.56 μm wavelength amounted to 7 dB/m. The optical loss minimum at 1.99 μm amounted to 0.12 dB/m.

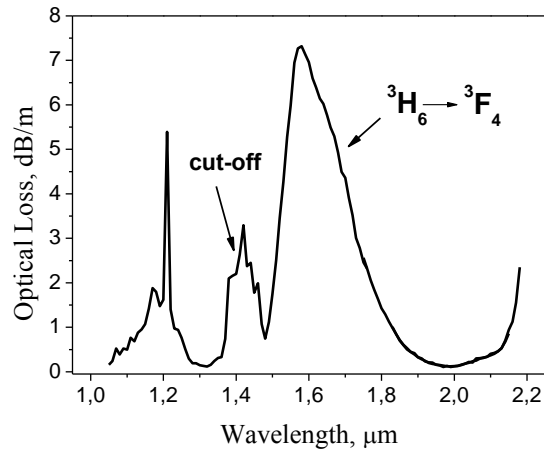


Fig. 2. Optical loss spectrum of the Tm-doped single-mode fiber. The peak at 1.43 μm is caused by the fiber cut-off. Spectral resolution is 5 nm.

Core-excitation of the fiber with an Er-doped fiber laser operating at 1.56 μm wavelength produced a character emission of Tm^{3+} in the range of 1.8-2 μm , corresponding to ${}^3\text{F}_4 \rightarrow {}^3\text{H}_6$ transition. The emission observed from the output end of the 10 m long fiber had a noticeable dependence on pump power. Its increase led to a rise of the emission intensity and a narrowing of its band-width (Fig. 3). At the same time the emission maximum experienced a blue-shift to 1.82 μm wavelength. The observed blue-shift was evidently caused by the saturation of the ground-state absorption when increasing the pumping rate.

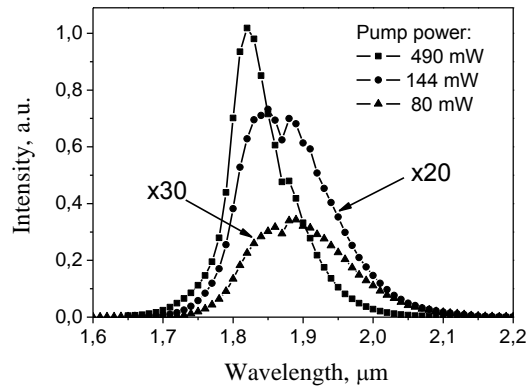


Fig. 3. ASE in the piece of fiber of 10 m length at different pumping rates. The curves corresponding to 144 and 80 mW of the pump power are multiplied by 20 and 30 times, respectively. Spectral resolution is 5 nm.

The dependence of the output power on the pump power is shown in Fig. 4 for the both fiber lasers. The unabsorbed pump power was about 40% for the short fiber laser and 10% for the long one.

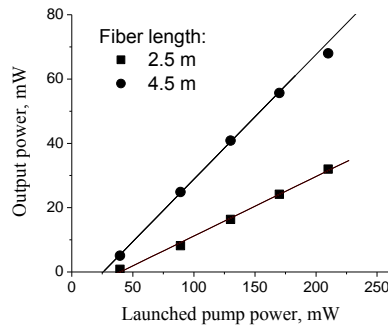


Fig. 4. The dependence of the output fiber laser power on the launched pump power for the two lasers of 2.5 and 4.5 m length of the active fiber.

The slope efficiency with respect to the launched pump power consisted of 26 and 37% for the short and long fiber lasers, respectively. The threshold was 40 and 25 mW for the short and long fiber lasers, respectively. Although the best slope efficiency of 37% is moderate, we suppose that the main reason for that are non-optimized laser parameters. Thus, the expected slope efficiency for this laser in the rough assumption of the complete absorbed pump conversion into the laser radiation is only ~60%. Optimization of laser parameters and components will allow further improvement of the efficiency.

The advantage of the 1.55 μm pumping is that usually no photodarkening with such pump wavelength is observed; in our experiments no change in the average output laser power during approximately one hour of operation has been observed.

The line-width of the laser emission was less than the experimental spectral resolution of 1 nm. The output spectra of both lasers also contain two spectral components at wavelengths of 1.84 and 1.884 μm (Fig. 5). Their intensities increased by a square law with the optical power of the central component at 1.862 μm . These symmetrical components were attributed to the four-wave mixing observed at relatively low powers due to operation in zero-dispersion region.

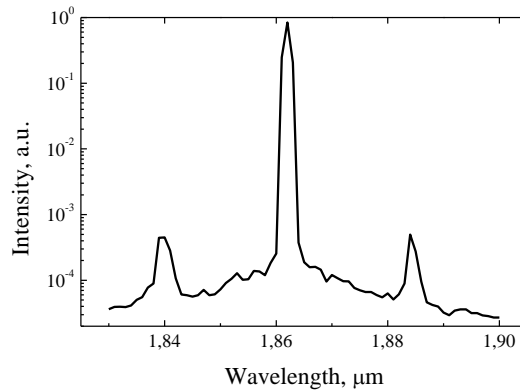


Fig. 5. The spectra of the output laser emission (70 mW of output power) of the fiber laser with the active fiber of 2.5 m length.

4. Theoretical analysis

The calculation of GVD has been based on the finite-element vectorial modelling of an effective refractive index of zero-order mode by the means of the COMSOL FEMLAB software package in combination with the Lumerical's MODE Solutions package. The

wavelength dependence of the bulk material refractive index for different concentrations of germanium has been approximated by Sellmeier's formula in correspondence with Ref [6]. The obtained solutions have been compared with the analytical results for a step-shape profile of germanium-concentration. The corresponding Maple computer algebra introduction can be found in [11].

As the experimental inputs, the Ge-concentration profile presented in Fig. 1 (and also, for convenience, in the inset of Fig. 6) and the measured cut-off wavelength at 1.43 μm wavelength have been chosen. The geometry of Fig. 1 has been supposed to be axially symmetrical and to be fitted by 11 radial layers describing the experimental decrease of the Ge molar concentration from 55% to 0% (i.e. to a pure SiO_2). The external layer of a pure SiO_2 has been assumed to extend to 15 micrometers. This geometry has been covered by a rectangular mesh with 500x500 points (i.e. an external SiO_2 ring has been inscribed into a square with the rest of a square filled by air). The fiber size has been defined from calculation of the measured cut-off wavelength at 1.43 μm . Numerically, the following criterion has been used: the cut-off wavelength corresponds to loss of confinement of the higher-order modes when the fiber is bended. The bending radius has been chosen to be equal to 1000 micrometers.

The GVD corresponding to the geometry shown in Fig. 1 (and also in the inset in Fig. 6) is presented by the solid curve with the grey area defining the uncertainty limits. It has been found, that the wavelength of zero GVD shifts into a longer wavelength region with the decreasing core radius and that this wavelength is quite sensitive to the core size. Such behaviour corresponds to the domination of the waveguiding effects in the vicinity of the second zero point of the GVD. This domination results from the comparatively small core radius and the very high numerical aperture of the fiber, resembling the tapered and microstructured fibers. The calculated zero dispersion wavelength equals to 1.87 μm for the given Ge distribution.

The interesting property of GVD in such fibers is that the third-order dispersion is comparatively small in the vicinity of zero-dispersion wavelength [12]. Moreover, the analysis suggests that the GVD can be made almost flat in both anomalous and normal regions within a broad wavelength range by sharpening of the Ge-concentration profile. As an example, two GVD curves for a step-like behaviour of the Ge concentration are shown in Fig. 7 by a solid (core radius 1.5 μm) and dashed (core radius 1.2 μm) curves. Suppression of the higher-order dispersion is especially important for mode-locked oscillators (see e.g [13]). The dashed curve in Fig. 7 demonstrates that the all-normal-dispersion (ANDi) regime of mode-locking [14,15] is feasible for very small core radii. Such regime is of interest for generation of the energy-scalable femtosecond pulses [16]. It has been predicted that ANDi fiber oscillators can be perfectly energy-scalable by fiber length scaling [17]. One can expect that the core size can also be enlarged without transition to the anomalous dispersion regime by fiber microstructuring [16]. The analysis of this possibility is under way now.

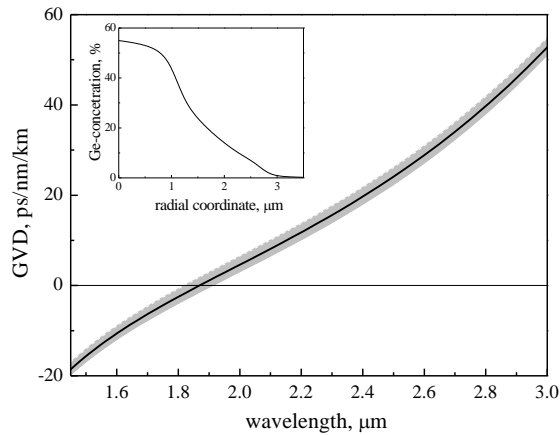


Fig. 6. Calculated dispersion of the fiber. The inset shows corresponding Ge distribution.

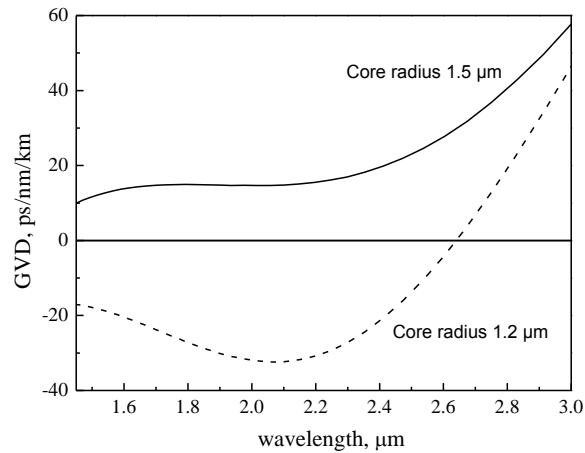


Fig. 7. Calculated dispersion of small-core step-index fibers with high GeO₂ doping.

5. Conclusion

We report the novel all-fiber laser based on the specially designed highly GeO₂-doped dispersion-shifted Tm-doped fiber, pumped at the 1.56 μm wavelength and lasing at the 1.862 μm wavelength with the slope efficiency up to 37%. The laser is based on the single-mode Tm-doped fiber with the 55GeO₂-45SiO₂ core fabricated for the first time by MCVD technique. The laser produces spectral side bands, which are additional to the laser line and result from the four-wave mixing owing to the high nonlinearity and to the shifted to the laser wavelength zero-dispersion-wavelength in this fiber. We analyze this phenomenon both, theoretically and experimentally. The demonstrated in this work possibility to optimize the dispersion of the fiber opens up new perspectives on the way towards obtaining ultrashort pulses directly from the resonator of the all-fiber dispersion compensated laser.

Acknowledgements

VVD and ITS acknowledge the support of the Norwegian Research Council (project 191614/V30), VLK acknowledges the support of the Austrian Fonds zur Foerderung der wissenschaftlichen Forschung (FWF project P20293).